Received: 3 February 2025 | Revised: 25 March 2025 | Accepted: 29 April 2025

DOI: 10.1111/ijac.15163

International Journal of Applied Ceramic Technology

RESEARCH ARTICLE

Sedimentation of particles in photopolymerizable suspensions

Vladislava Tomeckova | **Claudia Torres-Garibay** | **Brian J. Love** | **John W. Halloran**

Department of Materials Science and Engineering, University of Michigan, Ann Arbor, Michigan, USA

Correspondence
John W. Halloran, Department of Materials Science and Engineering, University of Michigan, Ann Arbor, MI, USA.
Email: peterjon@umich.edu

Abstract

An analytical centrifuge was used to examine the sedimentation of concentrated suspensions of refractory-grade silica particles in acrylate monomer mixtures. Depths for significant dilution or effective particle denudation were determined as a function of sedimentation time, and related to particle size distribution, particle volume fraction, the viscosity of the liquid, and the presence of thixotropic agents. Results for these dispersions are consistent with the Richardson–Zaki equation for hindered settling. The implications on three-dimensional (3D) printing of photopolymerizable suspensions are discussed.

KEYWORDS

3D printing, attenuation, ceramic/organic dispersions, photopolymerization, sedimentation, Stokes law

1 | INTRODUCTION

Photopolymerization of particulate suspensions is a popular method for three-dimensional (3DP) printing of ceramic green bodies by digital light processing DLP[1,2] vat stereolithography SLA.[3–5] Ceramic particles are commonly suspended as dispersions in liquids consisting of monomers, other reactive or nonreactive diluents, dispersants, and photoactive ingredients such as photoinitiators and absorbing dyes. These suspensions are photopolymerized layer by layer in a sequence of very many quite thin patterned layers, with the patterning accomplished with either a scanning laser or a digital mirror device. The photopolymerization can occur on the top surface at the air/suspension interface for "top-down" vat photopolymerization. Alternatively, the photopolymerization can occur in a layer of suspension adjacent to a transparent solid bottom for "bottom-down" photopolymerization.

Note that suspensions are inherently unstable. The particles gradually settle, creating a layer of sediment at the bottom and leaving a zone near the surface depleted of particles. The rate of sedimentation depends strongly on particle size, following the familiar Stokes law for very dilute suspensions with larger particles moving faster than smaller particles through the liquid. For very high particle volume fraction relevant for ceramic 3D printing, sedimentation rate does not follow the simple Stokes law of isolated particles. Rather, sedimentation from concentrated suspensions involves an ensemble behavior known as "hindered settling." Hindered settling is significantly slower than Stokes law settling, given that fluid motion is constrained by the larger number of particles over which fluid has to move. While suspensions of particles much smaller than 1.0 μm may remain suspended for weeks, certain applications, such as refractories, require the use of much coarser particles. Refractory-grade fused silica, commonly used for investment casting cores, often having particles larger than 50 μm.[6] These coarse particles can settle out of suspension rapidly and inconveniently during photofabrication.[7] Such refractory-grade silica powders are considered in this paper.

Sedimentation is not usually a practical concern for suspension processing in bulk, such as gel-casting. Large-scale sedimentation is easily avoided with mixing or

 © 2025 The American Ceramic Society.

agitation, which is a feature with some ceramic 3D printing devices. But sedimentation on a much shorter length scale may be important for 3D printing, because patterning is done on quite thin layers, typically 25–100 μm thick, either at the top surface or bottom surface of the suspension. Sedimentation over micron length scales can change the particle volume fraction in the near-surface or near-bottom regions. This can locally deplete the particle volume fraction near the top surface, relevant for top-down curing. For bottom-up curing, local sedimentation can enrich the volume fraction at the bottom surface. As the local suspension volume fraction determines the local green density, the cured layer can be inhomogenous on a fine scale. Perhaps a more significant impact of local changes in the particles volume fraction is a change the attenuation characteristics. The critical photopolymerization parameters of vary significantly with particle volume fraction,[8] which can result in errors in the important relationship between energy dose and depth of cure.[9]

To explore this, we have done a series of sedimentation experiments to address how particle volume fraction, particle size, liquid viscosity, and the addition of thixotropic agents affect sedimentation. We used analytical centrifugation to assess how compositional changes in the slurries affected their stability. We examined the effect of solids loading, the effect of size distribution, the effect of the viscosity of the monomer premix, and the role of additions of thixotropic agents. We expressed this in terms of hours of sedimentation, which is more convenient for these experiments to illustrate behavior, although somewhat unrealistic for actual practice.

2 | EXPERIMENTAL PROCEDURE

2.1 | Analytical centrifugation

Sedimentation experiments were done using an analytical centrifuge (LUMIsizer, LUM GmbH, Berlin Germany). An ampule of suspension was exposed to high *g*-forces in the centrifuge while the ceramic concentration was tracked as function of position using a CCD camera to monitor light transmission through the dispersion. The principles of the technique are presented by Minelli et al.[10] and Chen et al.[11] This instrument measures the vertical variation of optical extinction, which is proportional to the silica volume fraction. We report this as "volume fraction," but it should be noted that this is only the apparent volume fraction. We expect that optical extinction at any depth should depend both on the actual volume fraction and the local particle size distribution, as the scattering that causes the extinction depends on particle size. There is no direct information on differential sedimentation of the coarse and fine particles. Some segregation of the coarse particles has been reported[12,13] although at high volume fractions the sedimentation is well within the hindered settling regime. As a result, the fine particles with smaller Stokes velocities are pulled along by the large particles with faster Stokes velocities, decreasing the overall sedimentation rate.

The experiments were conducted at 1000 rpm, with 120 times normal gravity and converted by the instruments software to equivalent sedimentation profiles anticipated at normal gravity (1 g), so that a profile of ceramic volume fraction versus distance from the surface anticipated after sedimentation longer periods at normal gravity (1 g). Profiles were taken for equivalent real times of 1 h of sedimentation (30 s), 4 h (2 min), 12 h (6 min), and 24 h (12 min). The results report the apparent ceramic volume fraction as a function of depth (distance from the top surface), for various periods of equivalent sedimentation time.

2.2 | Materials

Formulations were prepared by mixing two monomers: bifunctional 1,6 hexane diol diacrylate, HDDA (SR238B, Arkema Sartomer) and tetrafunctional ethoxylated[4] pentaerythritol tetraacrylate, EOPETA (SR494, Arkema Sartomer USA). The monomers were used as-supplied, with no further purification. The suspension included 2.5% vol. of alkoxylated ammonium phosphate as a dispersant (Variquat CC-59, Evonik Goldschmidt Corporation), and filled with 30–60 vol% fused silica particles. The fused silica particles had irregular broken-glass shapes, with a density of 2.2 g/cm^3. The "fine" silica powder (Alfa Aesar Chemicals) had a particle size distribution was d_{10} = 2 μm, d_{50} = 7.1 μm, and d_{90} = 24.7 μm and a specific surface area of 5 m^2/g. The "coarse" silica powder had a d_{10} = 4 μm d_{50} = 26 μm d_{90} = 93 μm, with a specific surface area about 0.8 m^2/g. The suspensions were mixed for 2 days before using them. No photoinitiator was included here, as photopolymerization was not done. The small dose of photoinitiator has little effect on viscosity, so it should not affect sedimentation.

Suspensions were prepared with silica volume fractions varying from 30% to 60% v/v. Most dispersions had a HDDA/EOPETA ratio of 9/1, although one series had ratios varying from 9/1 to 0/10. We examined the effect of silica particle size distribution using suspensions made with a fine (d_{50} = 7 μm) and a coarser silica powder (d_{50} = 26 μm), and a bimodal powder consisting of 75 w/w% fine silica and 25 w/w% coarse silica. To explore the effect of initial

ceramic volume fraction, suspensions were prepared with 30, 40, 50, and 60 v/v%.

The influence of the viscosity of the suspension medium was explored two ways. For the standard diacrylate/tetraacrylate ratio of 9/1, we varied the temperature to change the viscosity. The viscosity of this Newtonian liquid was 9 mPa s at 20°C, 6 mPa s at 30°C, and 3 mPa s at 45°C. The corresponding viscosity of the 60 v/v% suspension of fine silica at a shear rate of 100/s was 1 Pa s at 20°C, 0.7 Pa s at 30°C, and 0.3 Pa s at 45°C. Another set of experiments were done at these temperatures using suspensions of the bimodal powder.

A second way to modify the viscosity was through the ratio of the more fluid diacrylate (9 mPa s) with the more viscous tetraacrylate monomer (108 mPa s). The viscosities of the mixtures were 11 mPa s for 9/1 HDDA/EOPETA, 16 mPa s for 7/3 HDDA/EOPETA, 26 mPa s for 5/5 HDDA/EOPETA, and 44 mPa s for 3/7 HDDA/EOPETA.

Thixotropic agents counteract sedimentation problems, which lead to softer sediments and slow settling by transforming the suspending liquid into a weak gel. We explored two thixotropes to be mixed into the suspensions. One was BYK 410, an organic thixotrope (BYK USA), which is a urea-modified polyurethane dissolved in methylpyrrolidone. The second was a hydrophobic fumed silica (HDK H18, Wacker Chemical Corporation) with a specific surface area of 200 m^2/g.

3 | RESULTS

We present the analytical centrifugation results as apparent volume fraction particles, inferred from the optical extinction, as a function of an equivalent time for sedimentation at 1 g. These are summarized in Table 1 as the depth at which the particle volume fraction has experienced significant dilution, from the original 60% v/v down to 50% v/v for both the fine silica and the bimodal mixture. Also shown are the depths at which the particles are effectively depleted, with less than 10% v/v remaining in suspension, after 12 h of sedimentation.

Figure 1 shows how the apparent ceramic volume percent changes with depth below the surface for a 60% v/v suspension of the 7-μm fine silica in the 9/1 diacrylate/tetraacrylate medium after sedimentation for 1–24 h. Note there is significant particle dilution (60% down to 50%) to a depth of 2.5 μm after 1 h, 5 μm after 4 h, 30 μm after 12 h, and 61 μm after 24 h of sedimentation. There is effective depletion of particles (below 10% solids) at a depth of 1 μm after 1 h, 4 μm after 4 h, 10 μm after 12 h, and 20 μm after 24 h. This suggests an apparent settling velocity for the 10% solids concentration point of 0.83 μm/h.

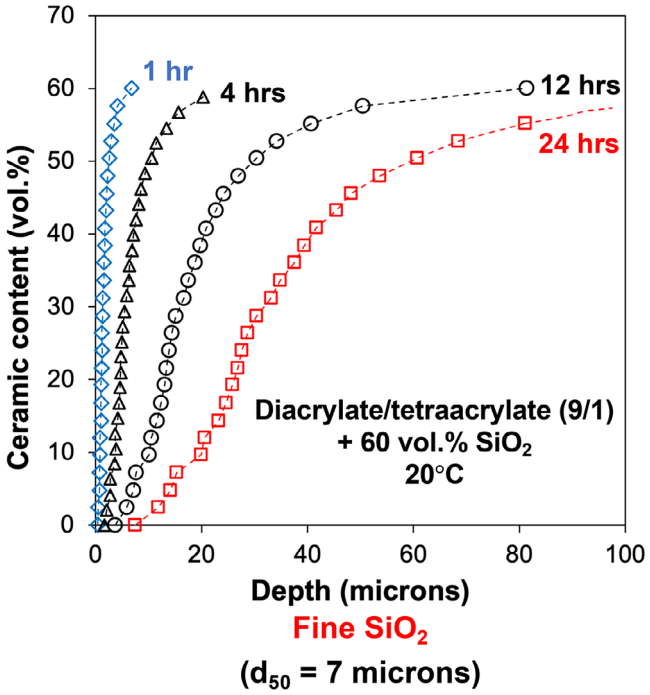


FIGURE 1 Ceramic volume percent versus depth and time for fine silica at 60 vol% particles at 20°C.

Figure 2 has comparable results for the bimodal silica, as ceramic volume percent changing with depth below the surface for a 60% v/v suspension of the bimodal silica in the 9/1 HDDA/EOPETA medium after sedimentation up to 24 h. Sedimentation is much faster for this bimodal powder, containing 25 wt% coarse (d_{50} = 26 μm) particles. Significant particle dilution (60% down to 50%) occurs to depth of about 25 μm after 1 h, 10 times deeper than the 7-μm powder in Figure 1. After 4 h, there is dilution to 50% v/v down to 90 μm. There is effective depletion (10% solids) at a depth of 8 μm after 1 h, 25 μm after 4 h and 60 μm after 12 h. For this coarser bimodal powder, the apparent settling velocity for the 10% solids concentration point of 2.3 μm/h.

As anticipated for concentrated suspensions under hindered settling, sedimentation is much faster for the less concentrated suspensions. Figure 3 shows the ceramic volume percent versus depth after sedimentation for the fine silica powder for the equivalent of 12 h at one gravity (actually 6 min in the centrifuge at 120 × g). Effective denudation depth (where the particle concentration is depleted down to 10% v/v) is 400 μm when the starting ceramic volume fraction is a relatively dilute 30% v/v. The 40% suspension has a denuded zone at 100 μm, while the 50% v/v starting suspension denuded depth is 31 μm and the 60% v/v suspension denuded depth is only 10 μm. Particle motion is much more difficult when the medium has to percolate around a much larger number of particles to

TABLE 1 Dilution and depletion depth versus sedimentation time.

	Depth to dilution from 60% to 50% (μm)				Depth to effective depletion (>10%; μm)			
Material	**1 h**	**4 h**	**12 h**	**24 h**	**1 h**	**4 h**	**12 h**	**24 h**
60 vol% fine	2.5	5	30	61	1	4	10	20
60 vol% bimodal	25	90	–	–	8	25	60	–
Fine powder 30%							400	
Fine powder 40%							100	
Fine powder 50%							31	
Fine powder 60%							10	
Bimodal 30%							500	
Bimodal 40%							200	
Bimodal 50%							100	
Bimodal 60%							28	
60 vol% fine + fumed silica thixotrope			26					
60 vol% fine + modified urea thixotrope			11					

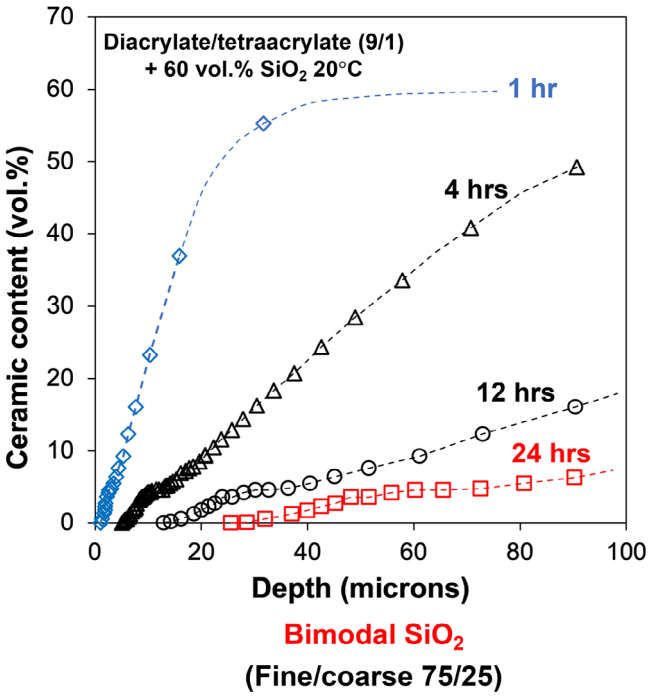


FIGURE 2 Ceramic volume percent versus depth and time for bimodal silica (fine/coarse 75/25) at 60 vol% particles at 20°C.

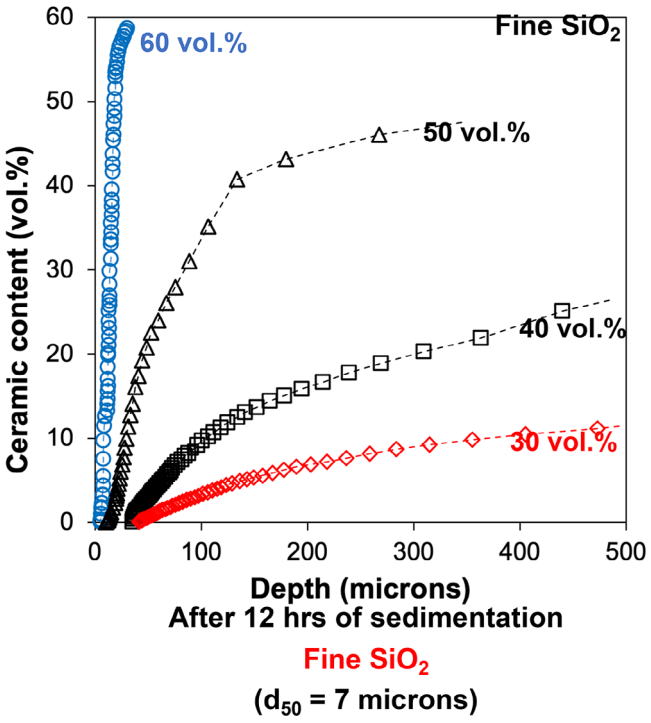


FIGURE 3 Ceramic volume percent versus depth after 12 h of sedimentation for fine silica (d_{50} = 7 μm) for varying volume percent particles at 20°C.

allow for sedimentation. Reducing the number of particles in the dispersion makes settling much faster.

Figure 4 compares the ceramic volume percent versus depth after the equivalent of 12 h sedimentation for suspensions of different concentrations. The addition of 25 wt% coarser silica makes sedimentation much faster, as expected. Again, there is the expected large effect of starting concentration, with the effective denuded zone (where only 10 vol% particles remain) at a depth of 28 μm for the most concentrated 60% v/v suspension, 100 μm for 50% v/v, 200 μm for 40%, and ~500 μm for suspensions with 30% v/v ceramic.

The 7 μm fine silica, the 21 μm coarse silica, and the bimodal mixture (75% fine/25% coarse) are compared in Figure 5, at 12 h of sedimentation of a 50% v/v suspension at 20°C. Using the 10 vol% "effected denudation" criterion

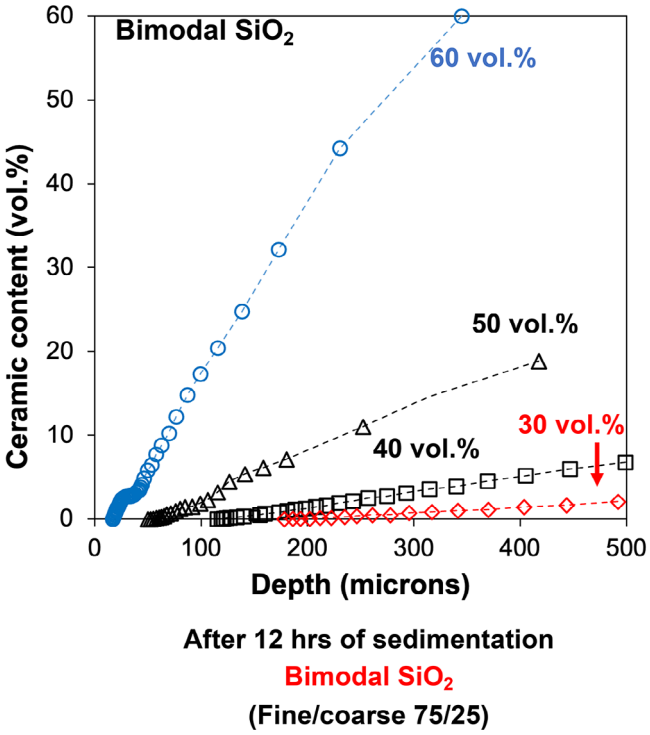


FIGURE 4 Ceramic volume percent versus depth after 12 h of sedimentation for bimodal silica (fine/coarse 75/25) for varying volume percent particles at 20°C.

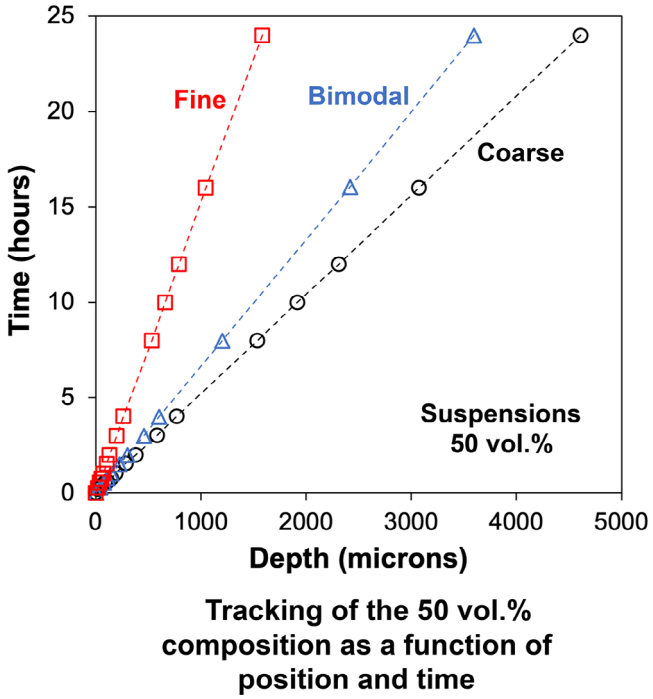


FIGURE 6 Location of the 50 vol% silica concentration as a function of time for fine, coarse, and bimodal size distributions at 20°C.

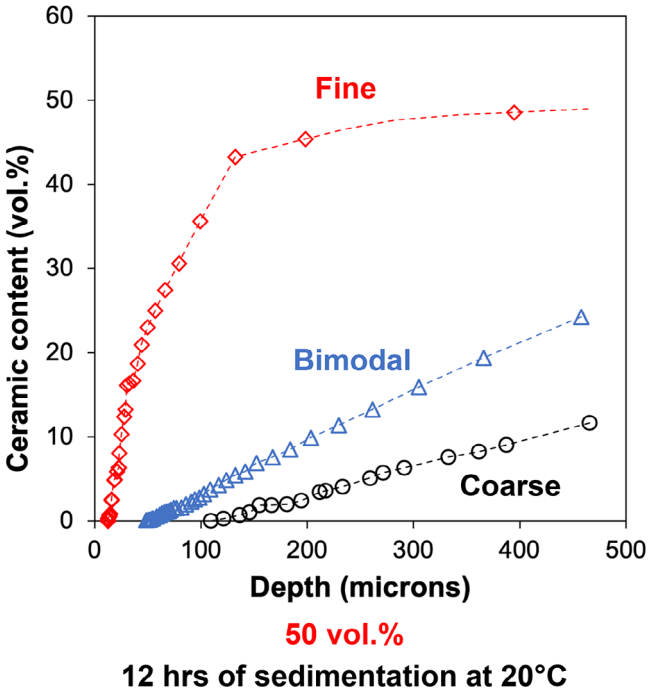


FIGURE 5 Effect of particle size on near-surface depletion after 12 h of sedimentation for 50 vol% silica suspension at 20°C.

as before, the fine powder has a denudation depth of about 20 μm while the coarse powder is denuded to a depth of 440 μm. The material has a layer that is clear of particles (0%) that is ~10 μm thick for the fine powder, 220 μm thick for the bimodal mixture, and 440 μm thick for the coarse powder.

The position as depth beneath the surface can be recorded versus the sedimentation time for any isoconcentration line. Figure 6 is an example, showing sedimentation time versus depth for the original 50% v/v isoconcentration for the fine, coarse, and bimodal powders, for suspensions prepared at a 50% v/v composition. For all three particle size types, the 50% v/v location changes linearly with time. The position of the 50% v/v line moves at 65 μm/h for the 7 μm fine silica, at 191 μm/h for the 26 μm coarse silica, and 149 μm/h for the bimodal powder.

The influence of the fumed silica thixotrope was small. Figure 7 shows volume fraction versus depth for 12 equivalent hours of sedimentation for the 60-vol% suspension of the 7 μm fine silica, with and without the addition of 0.75 wt% fumed silica thixotropic agent. This inorganic thixotrope had a small effect, reducing the 60%–50% dilution depth from 30 to 26 μm. The modified urea organic thixotrope at a dose of 0.75 wt% was much more effective. Figure 8 shows significantly slower sedimentation, compared with the suspension with no thixotrope, used at a dose of 0.75 wt% reduced the 60%–50% dilution depth from

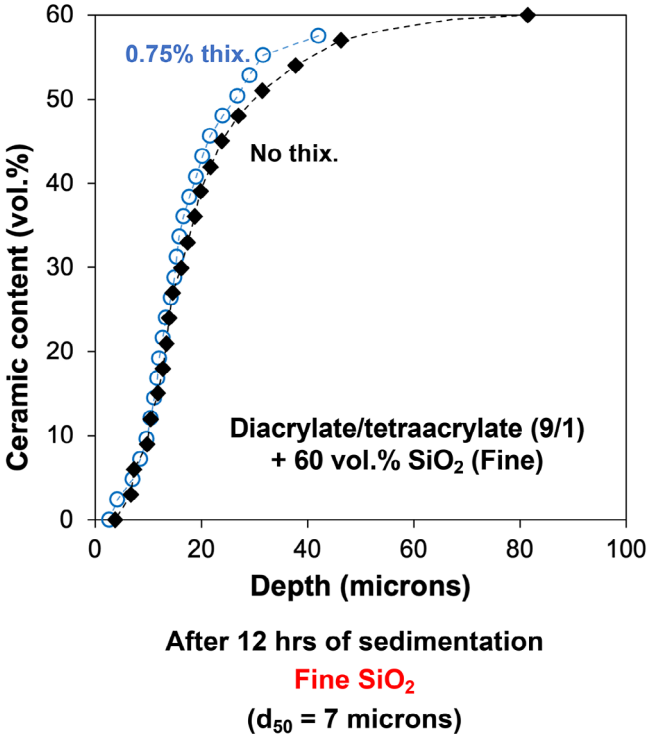


FIGURE 7 Ceramic content versus depth after 12 h sedimentation for fine silica influence of thixotropic agent.

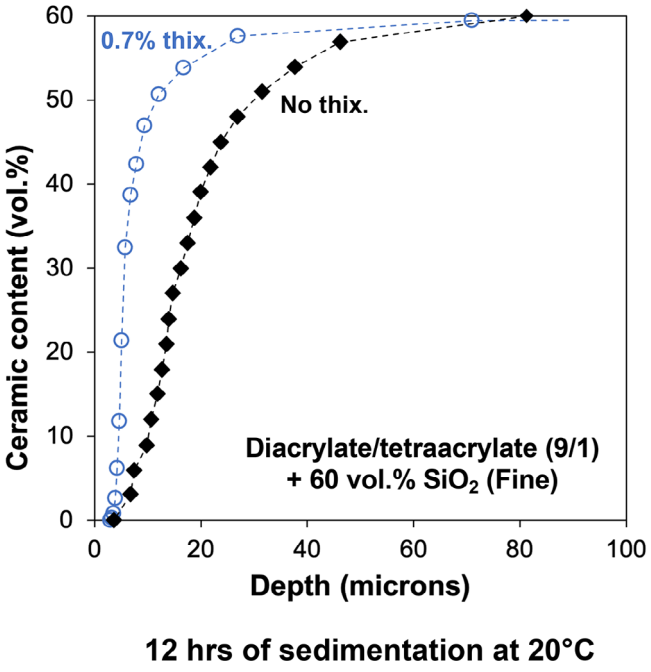


FIGURE 8 Effect of thixotropic agent on sedimentation of fine silica after 12 h.

30 μm to 11 μm. Larger additions of the urea thixotrope are increasingly effective for retarding sedimentation, as illustrated with the bimodal powder after 12 effective hours of sedimentation in Figure 9. This shows that after 12 h, the depth of effective denudation, where the silica fraction drops to 10% v/v, is at a depth of 60 μm with no added thixotrope, 34 μm with 0.75 wt% addition, 17 μm with 1.5 wt% addition, and only 13 μm with 3 wt% thixotrope.

A series of heated settling experiments were done to change the viscosity of the HDDA/EOPETA vehicle during sedimentation. Figures 10 shows the behavior for a 60% v/v suspension of fine silica for 12 effective hours of sedimentation. At 20°C, when the monomer viscosity is 9 mPa s, the fine volume fraction in Figure 10 is halved to 30% v/v at a depth of 14 μm. At 30°C, with monomer viscosity of 6 mPa s, that same ceramic volume fraction is found at a depth of 21 μm, and at 45°C, when the liquid viscosity is 3 mPa s, it is found at 40 μm. Figure 11 has the temperature dependence of the sedimentation for the bimodal powder. Again, the depth at which the concentration is reduced from 60% to 30% v/v is 72 μm at 20°C, 120 μm at 30°C, and 220 μm at 45°C. The amount of sedimentation varies linearly with viscosity in both cases, with a variation of 3.6 μm/h/mPa s for the 7 μm powder and 2.1 μm/h/mPa s for the bimodal powder.

One could also change the acrylate liquid viscosity by changing the relative amounts of the more fluid HDDA and more viscous tetraacrylate at one temperature. This is shown in Figure 12 for a 50% v/v suspension of fine silica after 12 h. Here, the depth for depletion to 30% v/v is 3 μm for pure tetraacrylate, with a liquid viscosity of 108 mPa s, 8 μm for the 3/7 HDDA/EOPETA (44 mPa s), 20 μm for the 5/5 mixture (26 mPa s), 43 μm for the 7/3 mixture (16 mPa s), and 79 μm for the standard 9/1 mixture (9 mPa s). Note that this change is not a simple linear function of viscosity, perhaps because the composition of the liquid differs.

4 | DISCUSSION

4The settling of particles in suspension is hindered by nearby particles, which interfere with the particle motion and restrict the backflow of the surrounding liquid. The hindrance effect is stronger at higher particles concentrations. It is common to express this hindered settling with the Richardson–Zaki relation.[14,15] This empirical equation relates the sedimentation velocity v to the particle volume fraction Φ of suspensions of nonagglomerating particles:

$$v = v_{\text{stokes}}(1 - \emptyset)^n = \frac{(\rho_p - \rho_L)}{18\eta} g d^2 (1 - \emptyset)^n \quad (1)$$

Here, ρ_p and ρ_L are the density of the solid ceramic particle and the monomer liquid, g is the gravitational acceleration, d is the diameter of particle, η is the fluid viscosity, Φ is the concentration of solid, expressed as

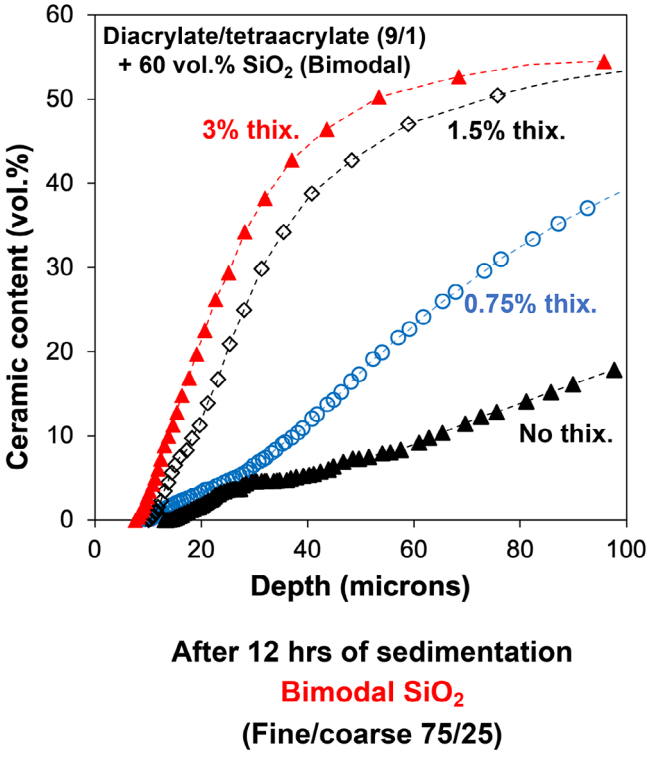


FIGURE 9 Effect of thixotrope concentration for bimodal silica after 12 h sedimentation.

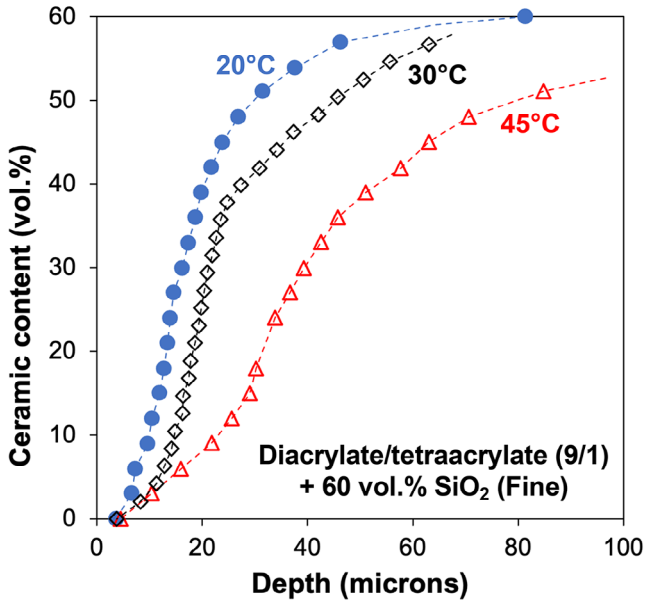


FIGURE 10 Effect of sedimentation temperature for ceramic concentration versus depth for 60 vol% fine silica after 12 h.

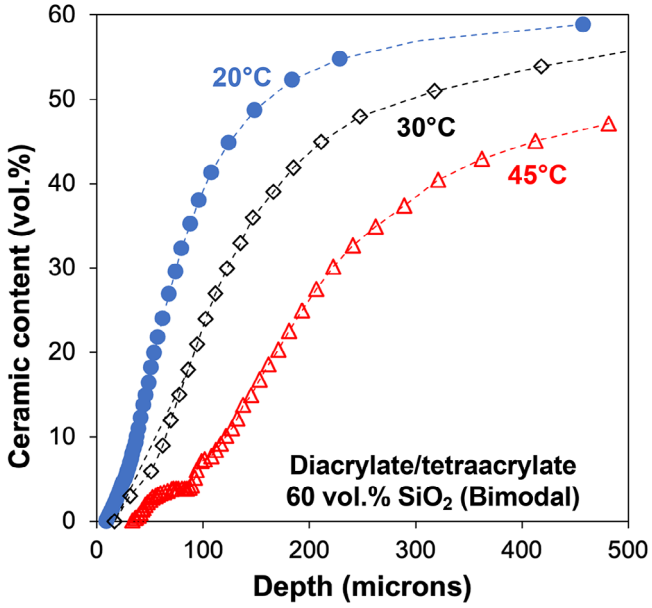


FIGURE 11 Effect of sedimentation temperature for ceramic concentration versus depth for 60 vol% bimodal silica after 12 h.

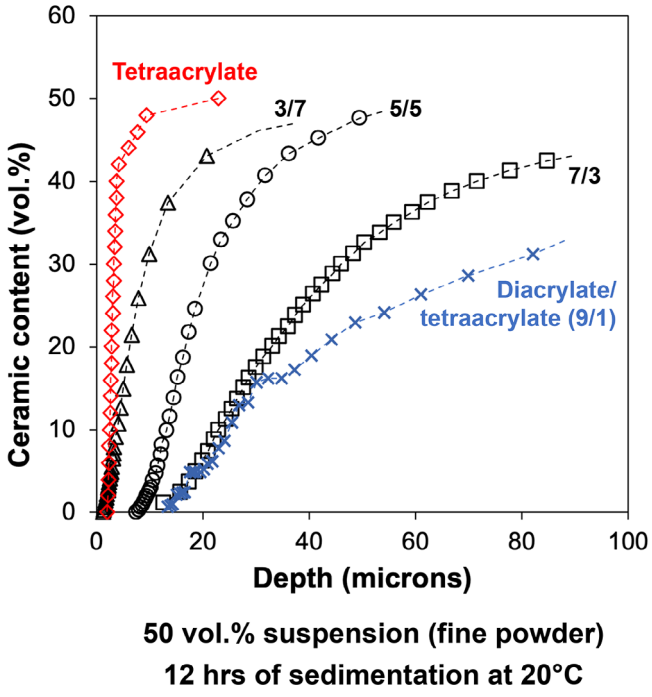


FIGURE 12 Ceramic concentration versus depth for 50% fine silica after 12 h sedimentation effect of diacrylate/tetraacrylate ratio.

volume fraction. The Richardson–Zaki power law coefficient, n, often has a value about 5 in the creeping flow regime. For aqueous suspensions of monodispersed silica nanospheres, Guo and Lewis[16] obtained $n = 4.63$. Bao et al.[17] modeled the stability of suspensions with a value of $n = 6.55$, using the experimental data of Al-Naafa and Sami Salim[18] for monodisperse and bidisperse hard spheres. Tseng and Wu[19] using gravity sedimentation of 1%–15% v/v alumina in water, noted a marked effect of hindered settling, with more dilute suspension settling much faster. Their values of the Richardson–Zaki coefficient were quite large, with $n = 17$.

The refractory silica powders in this study are quite polydispersed and have irregular, nonspherical shapes. We can estimate a value for the Richardson–Zaki coefficient using the time dependence of the denudation depth as an indicator of sedimentation velocity, and relating this to the particle volume fraction to obtain values for n. Table 1 has results for the depth for the effective depletion after 12 h. Using this depth to calculate sedimentation velocity for fine silica dispersed in the monomer, a least squares regression analysis so a logarithmic plot is a good straight line with a goodness of fit parameter $R^2 = 0.97$. The slope provides a Richardson–Zaki coefficient of $n = 5.9 \pm 0.8$. For the bimodal powder, the data in Table 1 are also linear in a logarithmic plot ($R^2 = 0.99$) with Richardson–Zaki coefficient of $n = 4.3 \pm 0.1$. These values are in the range which are reported for spherical particles.

There is some literature using analytical centrifuge to study sedimentation on comparable systems. Antonopoulou et al.[15] reported analytical centrifuge results for much finer silica 480 nm colloidal silica but in dilute suspensions, 1%–9% v/v. They noted significant hindered settling with higher concentrations, but they did not report a Richardson–Zaki coefficient. Sokola et al.[20] used centrifugal sedimentation to characterize the stability of photosensitive zirconia suspensions for DLP, although the emphasis was on the use of the instrument to characterize the zirconia powder.

4.1 | Implications for 3D printing

The entire build for a 3D-printed object may be many centimeters tall, but patterning by photopolymerization only occurs in an active layer that is one cure depth in thickness. The active layer is at the top of the suspension for top-down or the bottom of the suspension for bottom-up. If the ceramic particles are transparent and the refractive index differences between the medium and the particles is small (as in the case with SiO_2), the light attenuation in the photosuspension is dominated by absorption in the liquid by the photoinitiator or dyes. In this case, the light penetration and cure depth are decreased if sedimentation causes particle depletion in the curing layer. For transparent particles with a high refractive index (Si_3N_4, ZrO_2), attenuation can be dominated by light scattering, and the cure depth is larger than expected. For suspensions with absorbing particles (such as metal particles or SiC which is transparent in visible but opaque in UV), attenuation is dominated by absorption of the particles and depletion of particles by sedimentation can increase the cure depth. Changes the particle concentration even in a fraction of the layer thickness can lead to inaccurate prediction of the cure depth. If the material composition is not homogenous in this layer, the relation between cure depth and energy dose departs from the simple Beer–Lambert behavior of a homogenous layer.

To determine what energy dose (E_o) must be delivered to achieve the desired cure depth (C_d), 3D printers use the Jacob's Equation (9), which involves two photopolymerization parameters:

$$C_d = D_p \ln (E_o/E_c) \tag{2}$$

Here, the two photopolymerization parameters are D_p, the "depth of penetration," or sensitivity, and E_c is the critical energy dose needed for polymerization. Reliable and repeatable values of the sensitivity and critical energy dose are essential for accurate 3D printing by DLP or vat photopolymerization. Note that Jacob's equation assumes simple Beer–Lambert attenuation of the light, which implies that the material being illuminated is homogeneous.

These parameters can be related to the formulation of the suspension[8] in terms of the concentration of photoinitiator species c_{PI} and absorbing dye species c_{Dye}, the molar extinction coefficients of the photoinitiator (ε_{PI}) and dye (ε_{Dye}) and, relevant here, the volume fraction of suspended particles Φ. The relation can be expressed by Equation (2):

$$1/D_p = S(\Phi) + (1 - \Phi)\,A \tag{3}$$

Here, S is a scattering term, which depends upon the refractive index contrast between the particles and the liquid. This scattering term is a strong increasing function of volume fraction. The term A is an absorption term involving absorption of the light by the photoinitiators and dyes.

$$A = \left(\varepsilon_{PI} c_{PI} + \varepsilon_{Dye} c_{Dye}\right)$$

where $\varepsilon_{PI} c_{PI}$ is the product of the molar extinction coefficient of the photoinitiator and the molar concentration of the photoinitiator, and $\varepsilon_{Dye} c_{Dye}$ are the same terms for inert absorbing dyes.

When absorption dominates, as with silica which has a small refractive index contrast and less severe scattering, the reciprocal of the sensitivity D_p is proportional to sum of the absorption terms multiplied the volume fraction liquid (or $1 - \Phi$), as below

$$1/D_p \propto (1 - \Phi)\left(\varepsilon_{PI} c_{PI} + \varepsilon_{Dye} c_{Dye}\right) \tag{4}$$

Note that a decrease in near-surface particle volume fraction due to sedimentation increases the amount of absorption of the light, which decreases the sensitivity D_p. A change in the sensitivity will change the curing behavior, disturbing the relation between cure depth and

energy dose. Also, if the volume fraction changes in the region being cured, $\Phi(z)$ and the D_p value is not uniform in the curing layer, which violates the assumptions inherent in the Jacob's equation and leads to inaccurate prediction of cure depth. For higher refractive index ceramics, such as alumina or zirconia, Equation (2) can be dominated by the scattering term S. If local sedimentation reduces the volume fraction in the region being cured, $\Phi(z)$ and the D_p value can be smaller than expected.

The critical energy dose is proportional to the volume fraction solids and the ratio of the dye and photoinitiator concentrations,[8] as shown in Equation (5).

$$E_c \propto (1-\Phi)\left(c_{Dye}/c_{PI}\right) \tag{5}$$

Note that sedimentation reducing the near-surface particle volume fraction raises the critical energy dose E_c, which also affects the curing response.

Near-surface particle depletion of ~10 μm, a fraction of a layer thickness, can change the critical energy dose and depth of penetration, and lead to an unexpected or non-Beer–Lambert cure profile. This is of particular importance in absorption-dominated cases (low refractive index contrast with high PI or dye concentration), where near-surface region can have much shorter D_p.

With transparent particles, a lower solid content locally decreases D_p as the local concentration of absorbing dyes and photoinitiator increases when not diluted by the ceramic particles. With low refractive index, transparent particles, the D_p is dominated by absorption of the liquid, which is more pronounced in the region cleared particles by settling. For top-down, 3D printing, the smaller D_p in the clarified zone can make the actual cure depth smaller than expected. For higher refractive index particles, the sensitivity D_p can be dominated by particle scattering, so a near-surface region cleared of particles can have a larger D_p, again making the cure depth different from the expected value. The converse is true for bottom-up, 3D printing.

Sedimentation can also create problems at a larger scale. Vat photopolymerization has suspension in the vat for periods of many hours, which implies the possibility that big particles settle to bottom of vat. This creates sediment in bottom, which can be mechanically inconvenient. Vat-scale sedimentation also decreases particle concentration remaining in rest of the suspension. For hollow objects, uncured suspensions inside the object can create an interior sediment, which complicates clearing after the build.

The top surface of vat has some stirring from the recoat blade. For some top-down methods fresh suspension is supplied during recoating. Traditional dip methods supply suspension from near-surface of the vat by dipping the build a short distance from the surface so surrounding suspension flows in. For these top-down methods, the near-surface suspension may also be depleted of particles by sedimentation. Bottom-up methods, supply fresh suspension to active region suspension near the bottom, which can be enriched in particles that have settled. Both approaches can complicate the composition of the recharged regions now awaiting cure in the next layer.

5 | CONCLUSIONS

Sedimentation rate of concentrated suspensions of silica powders in acrylate monomer solutions is slower for higher solids concentration, consistent with hindered settling behavior. For a finer silica powder, with 7 μm median particles, the depth from the surface where the particles are mostly depleted (10% v/v) falls at a rate of 33 μm/h for a more dilute 30% v/v suspension, but only at a rate of 0.83 μm/h for a more concentrated 60% v/v suspension. A bimodal powder mixture, containing 25 wt% of a coarser silica (with 26 μm median diameter) settles faster. more quickly. The velocity of the 10% v/v depletion depth is 41.7 μm/h for the 30% v/v suspension, and 2.3 μm/h for the more concentrated 60% v/v suspension.

The variation of settling velocity with volume fraction solids can be fit to the Richardson–Zaki equation with and Richardson–Zaki exponents $n = 5.9 \pm 0.8$ for the fine 7 μm powder and $n = 4.3 \pm 0.1$ for the bimodal powder.

The position of 50% v/v isoconcentration lines is linear functions of time, faster for the coarse powder, slower for the bimodal powder, and slowest for the finer powder.

When the viscosity of the acrylate liquid is changed with temperature, the settling velocity is faster as the viscosity decreases. The change in settling velocity is a linear function of viscosity. Changing viscosity of the liquid by changing the relative amount of the more fluid bifunctional monomer and the more viscous tetrafunctional monomer also changes the settling velocity in proportion to the liquid viscosity.

The addition of a fumed silica thixotrope had only a small effect. An organic urea-modified polyurethane thixotrope was effective for slowing sedimentation.

Sedimentation on a micron scale can affect the photopolymerization sensitivity and critical energy dose, by changing the volume fraction in the near-surface region, this can make the material inhomogeneous, leading to errors in the relationship between cure depth and energy dose.

ACKNOWLEDGMENTS

We thank Steven J. Norton and Joseph C. Tucker for experimental assistance.

ORCID

John W. Halloran https://orcid.org/0000-0002-1913-6886

REFERENCES

1. Stampfl J, Schwentenwein M, Homa J, Prinz, Fritz B. Lithography-based additive manufacturing of ceramics: materials, applications, and perspectives. MRS Commun. 2023;13:786–84.
2. Sokokola P, Kalina M, Smilek J, Ptacek P, Krouska J Salamon D, et al. Kinetic stability and rheological properties of photosensitive zirconia suspensions for DLP. Ceram Int. 2023;49:18502–9.
3. Li YH, Sheng PF, Lin LF, Wang L, Lu D, Lin K, et al. Vat photopolymerizaton versus conventional colloidal processing methods in structural ceramics: progress, challenges, and future perspectives. Addit Manuf Front. 2024;3:200110.
4. Halloran JW. Ceramic stereolithography: additive manufacturing for ceramics by photopolymerizarion. Annu Rev Mater Res. 2016;46:19–40.
5. Leite de Carmago I, Morais MM, Fortulan CA, Branciforti MC. A review of the rheological behavior and formulations of ceramic suspensions for vat photopolymerization. Ceram Int. 2021;92:11906–21.
6. Jin F, Li QL, Yang K, Qiu YX, Liu XG, Liang JJ, et al. Optimization and applications of high solids loading stereolithograpy 3D printing ceramic cores slurry. Ceram Int. 2024;50:3574–83.
7. Bae C-J, Halloran JW. A segregation model study of suspension-based additive manufacturing. J Eur Ceram Soc. 2018;38:5160–66.
8. Tomeckova V, Halloran JW. Predictive models for the photopolymerization of ceramic suspensions. J Eur Ceram Soc. 2010;30:2822–40.
9. Jacobs PF. Rapid prototyping and manufacturing – fundamentals of stereolighography. Society of Manufacturing Engineers, Southfield, Michig; 1992.
10. Minelli C, Kestens V, Babick F, Lerche D. Particle separation techniques: fundamentals, instrumentation, and selected applications. Elsevier Ltd, Amsterdam, Netherlands; 2022.
11. Chen H, Hia X, Fairweather M, Hunter TN. Characterization of the sedimentation of bidisperse colloidal silica using analytical centrifugation. Adv Polym Technol. 2023;34:103950.
12. Bae C-J, Halloran JW. Concentrated suspension-based additive manufacturing – viscosity, packing density, and segregation. J Eur Ceram Soc. 2019;39:4299–306.
13. Bae C-J, Ramachandran A, Halloran JW. Quantifying particle segregation in sequential layers fabricated by additive manufacturing. J Eur Ceram Soc. 2018;38:4082–4088.
14. Richardson JF, Zaki WN. The sedimentation of a suspension of uniform spheres under conditions of viscous flow. Chem Eng Sci. 1954;3(2):65–73.
15. Antonopoulou E, Rohmann-Shaw CF, Sykes TC, Cayre OJ, Hunter TN, Jimack PK. Numerical and experimental analysis of the sedimentation of spherical colloidal suspensions under centrifugal force. Phys Fluids. 2018;30:030702.
16. Guo JJ, Lewis JA. Effects of ammonium chloride on the rheological properties and sedimentation behavior of aqueous silica suspensions. J Am Ceram Soc. 2000;82:266–72.
17. Bao ZL, Huan DM, Yu H, Wang YQ, Chang QB. A model for predicting the stability of ceramic suspensions. Ceram Int. 2024;50:1990–99.
18. Al-Naafa MA, Sami Salim M. Sedimentation of monodisperse and bidisperse hard-sphere colloidal suspensions. AIChE J. 1992;38:1618–30.
19. Tseng WJJ, Wu CH. Sedimentation, rheology and particle packing structure of aqueous Al_2O_3 suspensions. Ceram Int. 2003;29:821–28.
20. Sokola P, Ptacek P, Kalina M. Stability of photosensitive zirconia suspensions as a factor for rheological measurements. In: Presented at processing and properties of advanced ceramics and glass workshop, Vrsatske Podhradie, Slovakia 16–18 Oct 2024.

How to cite this article: Tomeckova V, Torres-Garibay C, Love BJ, Halloran JW. Sedimentation of particles in photopolymerizable suspensions. Int J Appl Ceram Technol. 2025;22:e15163. https://doi.org/10.1111/ijac.15163